UNIVERSITY OF TARTU

FACULTY OF SCIENCE AND TECHNOLOGY

INSTITUTE OF PHYSICS

Andrei Kovaljov

DEVELOPMENT OF METHOD FOR DETERMINATION OF MINIMAL DETECTION ABILITY OF BISMUTH GERMANIUM OXIDE GAMMA DETECTOR

Bachelor's thesis (12 EAP)

Supervisors:

Alan Henry Tkaczyk, Ph.D.

Dmitrii Vakhtin, Ph.D.

Tartu 2016

Table of Content

1 Summary

The aim of this thesis was to find experimentally the minimal activity of Co-60 and Cs-137 isotopes carried by a person walking at a speed of about 5 km/hour that can be detected by spectroscopic gamma-ray detectors placed in the geometry of a pedestrian portal with less than 1 false alarm in 24 hours. On order to achieve it, following steps were made:

1. The ability of MCNP code to calculate responses of scintillator-based detectors was tested. The results were confirmed by direct measurements.

2. Experimental setup with BGO-based gamma-detector and Co-60 and Cs-137 gamma-sources was constructed.

3. Feasibility of using spectroscopic scintillator detectors as part of security portals operating in real time has been confirmed.

4. The minimal detectable activities of Co-60 and Cs-137 in the case of using one detector were experimentally determined.

The results show that minimal detection ability of only 1 BGO detector is enough to detect minimal activity of Co-60 that is not dangerous to environment determined by IAEA norms, and is not enough to detect minimal activity of Cs-137.

CERCS codes: P220 Nuclear physics, T160 Nuclear engineering and technology.

2 Kokkuvõte

Käesoleva töö eesmärgiks oli katseliselt, kiirusega 5km/tunnis kõndiva inimese kantud Co-60 ja Cs-137 gamma-allikate minimaalsete aktiivsuse väärtuste leidmine, mis on avastatavad jalakäijate turvavärava geomeetriale vastavalt asetatud spektroskoopilise gammadetektorite abil nii, et 1 valehäire esineks rohkem kui 24 tunni jooksul. Selle saavutamiseks teostati järgnev:

1. Katsetati programmi MCNP sobivust stsintillatsioon- detektorite koste väljaarvutamiseks. Arvutustulemused said kinnitust otsemõõtmistel.

2. Koostati eksperimentaalne skeem, mis koosnes BGO-l põhinevast gamma-detektorist ning Co-60 ja Cs-137 gamma-allikatest.

3. Tõestati spektroskoopiliste stsinillatsioon-detektorite sobivus kasutamiseks reaalajas töötavates turvaväravates.

4. Määrati eksperimentaalselt Co-60 ja Cs-137 allikate aktiivsuste minimaalsed avastamisväärtused ühe detektori kasutamisel.

Tulemused näitavad, et juba ühe BGO detektori avastamisevõimest piisab Co-60 allika, mille gamma-aktiivsus ei ületa IAEA poolt määratud ohutuspiiri, avastamiseks, kuid jääb siiski väheseks IAEA ohutusnormidele vastava aktiivsusega Cs-137 allika avastamiseks.

CERCS koodid: P220 Nuclear physics, T160 Nuclear engineering and technology.

3 Introduction

Unlike 70-80 years ago, when scientists were developing first nuclear weapons, nowadays society is well informed of the harm that ionizing radiation may cause. Due to intensive technical development and unstable situation in some regions of the world, it is clearly understandable that the topic of radiation protection is going to be on top of the society's agenda. In order to prevent illegal dissemination of radioactive materials more efficiently, new detecting systems are being developed. While small hand-held radiation detectors are often used to check on a particular threat, stationary radiation portals are much more efficient in places with a lot of human and transport traffic (such as seaports, railway stations, airports, customs and border crossings, etc.). These radiation portals may have different sizes and design, all of them contain the following main components:

1. An energy-sensitive radiation detector.
2. An amplifier that amplifies the signal to levels suitable for modern electronics.
3. Electronics to process signals produced by the detector to form an energy spectrum (e.g. a multichannel analyzer).
4. Data readout device that transfers the digitized information to computer or screen.

Development of reliable electronics and powerful data analysis algorithms made possible fully automated standalone radiation portals that are widely used at border and Customs checkpoints worldwide. One important requirement for pedestrian radiation portals is that they have very low false alarm rate, so that for example they do not react on “legitimate” medical isotopes that people may carry in their bodies. This is usually achieved nowadays by introducing spectroscopic channel that can select only isotopes of interest while suppressing any variations in the background [1].

The next logical step will be integration of pedestrian radiation portals into a broader security infrastructure together with a new generation of automatic threat detection technologies, such as security radars [2].

The main goal of this bachelor thesis was to find experimentally the minimal activity of Co-60 and Cs-137 isotopes carried by a person walking at a speed of about 5 km/hour that can be detected by spectroscopic gamma-ray detectors placed in the geometry of a pedestrian portal with less than 1 false alarm in 24 hours.

This work was supported by APSTEC Systems, which has a test laboratory in Tartu. APSTEC took part in formulating the goals of the work and also provided operational gamma-rays detectors based on BGO (Bismuth germanium oxide) crystal together with data collection software. It also provided a two

weeks-long training course in operating the detector, analyzing the obtained spectra, and modeling gamma-spectra with MCNP code.

4 Theoretical aspects of detection of gamma-rays

4.1 Interaction of photons with matter

The main physical mechanisms of gamma-rays interaction with matter that are important for understanding the obtained spectral shapes are Compton scattering, photoelectric effect and pair-production process.

In the Compton effect, the photon is scattered from an electron that is essentially not bound to an atom. Because the scattering angle can vary from 0 to 180 degrees, there is a range of energies that can be transferred from the photon to the recoiling electron:

$$\lambda' - \lambda = \lambda k \, [1 - \cos(\theta)] \qquad (1)$$

where λ is initial wavelength, λ' is wavelength after scattering, θ is scattering angle and λk is Compton wavelength. The scattered photon survives and carries off the remainder of energy. It is the recoiling electron that loses energy by ionizing the detector material. Consequently, the charge collected from the detector will yield a distribution of pulse amplitudes at the preamplifier output up to some maximum pulse height. There is a statistical probability that each Compton scattering event has an approximately equal chance to produce a pulse with any height up to this maximum. Thus, Compton events will provide a broad low-energy continuum in the spectrum ([3], pp. 87-94).

In the photoelectric effect, the photon transfers all its energy to an electron in the detector and disappears. The electron loses energy by causing further ionization of the detector material. Depending of the detector type (semiconductor, scintillation) this ionization is converted into a signal by an appropriate mechanism ([3], pp. 83-87)

During the pair-production process, the gamma-ray photon enters the detector, creates an electron-positron pair and disappears. All the energy of the initial photon is transferred to the electron-positron pair:

$$E_0 + p = h\nu - 2m_0c^2 \qquad (2)$$

Both the positron and the electron lose energy by causing ionization of the atoms in the detector. Because the positron is moving slowly enough, it can be captured by a free electron, and the two can combine. In this annihilation of the positron with an electron, both particles disappear, and their rest masses (511 eV each) are converted into two photons traveling in opposite directions. Since both these photons can lose all their energy in the volume of the detector, or one of both of them can escape, three peaks are appear in the measured spectrum: the main one (full energy peak - both photons interact with

crystal), single escape peak (only one interacts with the matter, another escapes) and double escape (both photons escape without interaction). ([3], pp. 95-97)

4.2 Detecting gamma-rays by scintillator-based detectors

The key element of any gamma-detector is energy-sensitive radiation detector (ESRD). The most important qualities of ESRD are [4]:

1. Percent efficiency (also known as "efficiency") – the percentage of events (decays) detected relative to all the source's decays in the same time interval. It mostly depends on size and density of ESRD; and the distance (and obstacles) between ESRD and gamma source.

2. Peak-to-total ratio (or "peak-to-Compton ratio") is determined by summation of the counts for all channels under the photo peak and dividing by all counts observed in the entire spectrum. The ratio generally decreases with increasing energy of the gamma ray. Good peak-to-total ratio allows one to easily separate the photo peak from the background and Compton scattering.

3. Resolution – the ability of detector to resolve two peaks close in energy to each other. Wider peaks mean more error. Resolution is defined by measuring the width of the peak halfway to the top (Full Width at Half Maximum or FWHM) and dividing by the energy of the photo peak (E_0):

$$\%\text{Resolution} = \frac{FWHM}{E_0} \times 100\% \qquad (3)$$

Currently, due to low cost and good efficiency, the most widespread gamma detector among radiation portals is polyvinyl-toluene (PVT) plastic scintillator. However, it has very poor energy resolution, so it cannot identify the radioactive isotope and is thus not used in spectroscopic gamma-ray detectors, which must be able to distinguish between naturally occurring isotopes, medical isotopes etc.

On the other end of the price scale are semiconductor high purity Germanium (HPGe) detectors, which have excellent energy resolution, but poor efficiency at higher energies. HPGe are rarely used in pedestrian portals due to their very high cost and the need of cooling, and because one has to wait for a long time to collect even a few events before the detector's excellent energy resolution can be used.

Typically, spectroscopic portals use NaI type scintillating crystals, which have medium energy resolution and medium efficiency. In this work another type of scintillator crystals was used: Bismuth germanium oxide (BGO), which has slightly worse energy resolution than NaI of the same size, but a much better peak-to-Compton ratio([3], [5], [6]).

4.3 Modeling gamma-spectra using MCNP code

MCNP[1] is a Monte-Carlo code created in Los-Alamos National Laboratory in 1960s with the primary goal of calculating criticality parameters of fission assemblies. Later it became a general purpose neutron and gamma transport code that is widely used to calculate detector responses and estimate shielding efficiency.

MCNP calculations are based on extensive data libraries that are supplied together with the code.

An MCNP problem is set up by writing a text file containing instructions describing geometry, materials, radiation sources and detectors. In this Thesis we used the gamma-ray detection subset of MCNP, which allows one to simulate the pulse shape spectra of arbitrary gamma-sources.

Below is an example of a text file containing instructions to calculate the response of a BGO-based scintillator detector to Cs-137 source.

```
c ------------------------------------------------------------------------------
c ********** Response function calculation
c ********** (C) Andrej Kovalyov, APSTEC Systems, 2015
c ------------------------------------------------------------------------------
c ********** CELLS
1 0  (-1:2:-3:4:-5:6)                    imp:p=0 $ outside of the room
2 1 -0.00123 1 -2 3 -4 5 -6 #3           imp:p=1 $ air in the room
3 2 -7.13 -10 11 -12 trcl=1              imp:p=1 $ BGO crystal

c ------------------------------------------------------------------------------
c ********** SURFACES
c *** Room walls
1 PX -100            $ YZ plane
2 PX  100            $ YZ plane
3 PY -100            $ XZ plane
4 PY  100            $ XZ plane
5 PZ -100            $ XY plane
6 PZ  100            $ XY plane
c
c *** 3inch X 3inch cylinder (BGO crystal)
10 CY   3.81         $ cylinder
11 PY   0            $ XZ plane
12 PY   7.62         $ XZ plane

c ------------------------------------------------------------------------------
c ********** COORDINATE TRANSFORMATIONS
TR1 0.0 50.0 0.0                              $ shiftX, shiftY, shiftZ
c
c ------------------------------------------------------------------------------
```

1 http://www.iaea.org/inis/collection/NCLCollectionStore/_Public/18/044/18044302.pdf

```
c ********** MATERIALS
m1 7014   0.800   8016  0.200              gas=1        $ Air in room
m2 83209  0.211  32000  0.158 8016   0.631             $ BGO crystal
m3 14000 -0.200   8016 -0.495 20000 -0.286 1001 -0.019  $ Concrete
m4 6000   0.333   1001  0.667                           $ Polyethilene
c
m5    1001 1                                           $ H
m6    6000 1                                           $ C
m7    7014 1                                           $ N
m8    8016 1                                           $ O
m9    9019 1                                           $ F
m11  11023 1                                           $ Na
m12  12000 1                                           $ Mg
m13  13027 1                                           $ Al
m14  14000 1                                           $ Si
m15  15031 1                                           $ P
m16  16000 1                                           $ S
m17  17000 1                                           $ Cl
m19  19000 1                                           $ K
m20  20000 1                                           $ Ca
m21  21000 1                                           $ Sc
m22  22000 1                                           $ Ti
m23  23000 1                                           $ V
m24  24000 1                                           $ Cr
m25  25000 1                                           $ Mn
m26  26000 1                                           $ Fe
m27  27000 1                                           $ Co
m28  28000 1                                           $ Ni
m29  29000 1                                           $ Cu
m30  30000 1                                           $ Zn
m32  32000 1                                           $ Ge
m33  33075 1                                           $ As
c
c ---------------------------------------------------------------------------
c ********** GAMMA SOURCE
c http://ie.lbl.gov/toi/nucSearch.asp
c
SDEF ERG=D1 POS 0 0.01 0 par=2         $ Gamma source location
c
c *** Line energies in MeV
SI1 L 0.28353 0.661657
c *** Relative line intensities
SP1 0.00058 85.1
c
c ---------------------------------------------------------------------------
c ********** GENERAL SETTINGS
MODE P                         $ Account for photons
NPS 1000000000                 $ Number of photons to emit
```

```
c
c -------------------------------------------------------------------------------
c ********** OUTPUT OPTIONS
print
prdmp j j j 1 j
c
c -------------------------------------------------------------------------------
c ********** TALLIES
f8:p 3                        $ pulse high distribution in cell 3
ft8 GEB 0.0 0.075 0.0         $ BGO energy resolution: FWHM = a+b*sqrt(E+c*E^2)
e8   0 3999I 4.0              $ energy range and energy bins
c
```

Meaning of different sections are explained in the comments in the text.

Figure 1 shows results of calculations of responses of the BGO detector to a number of important gamma-emitting isotopes that are widely used in industry.

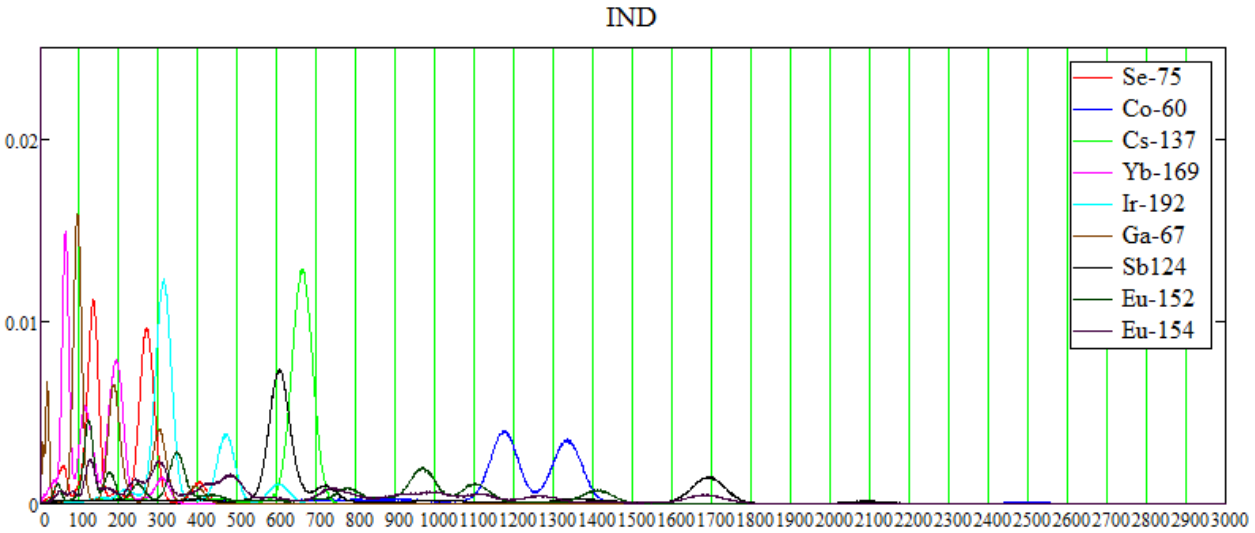

Figure 1. Calculated responses of the 3x3 inch BGO detector to some gamma-emitting isotopes

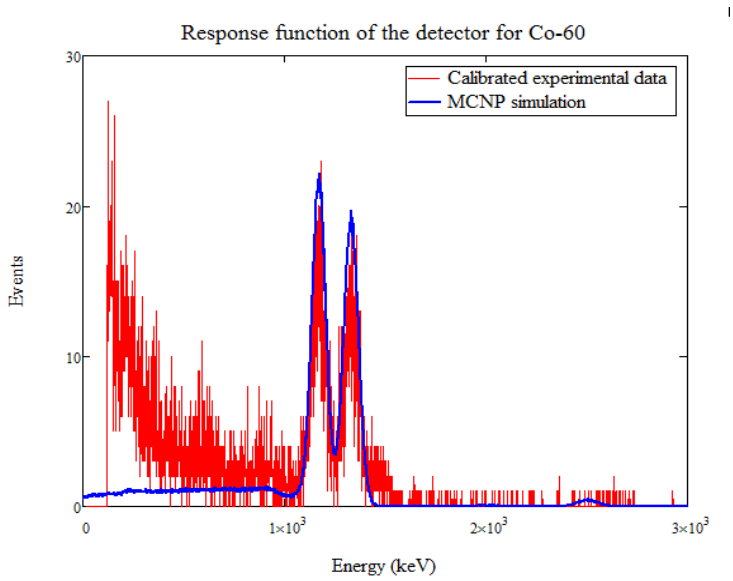

Figure 2. Comparison of the measured (red line) and calculated (blue line) spectra of Co-60 for 3×3 inch BGO gamma-ray detector.

Figure 2 shows comparison of the measured and calculated spectra of Co-60 for 3×3 inch BGO gamma-ray detector. Thus, MCNP allows one to calculate the response of the given type of gamma-detector to any isotope in realistic assumptions about the detection geometry and the surrounding materials.

5 Experimental work

5.1 Description of the equipment

In this work the following equipment was used:

1. APSTEC's gamma detector with cylindrical ∅3×3 inch bismuth germanium oxide (Bi4Ge3O12 or BGO) crystal as energy-sensitive radiation detector, HAMAMATSU R6233-01 photo multiplier with voltage divider, and custom made digital electronics with fast amplitude-to-digital converter.
2. USB cable for power supply of the detector and data transmission.
3. Personal computer for data storing and processing.
4. 2 wooden rectangular rulers for determination of fact that the whole detector is strictly perpendicular to the path of source and for determination of distance between them.
5. 2 paper rulers (1 m long) for measurement source's positions on their path.
6. 2 tables, where the whole experiment was made.

5.2 Description of gamma-sources

Due to pretty high threshold energy of the BGO detector, it can not effectively detect gamma rays with energy less than 200 keV, which decreases the variety of detectable radioactive isotopes. However, there are still around 23 high abundance isotopes that BGO detector is able to identify (see Appendix A). Two of them were available in university of Tartu for experiments:

1. Cs-137 with current activity 8.81(7) kBq.
2. Co-60 with current activity 27.83 (27) kBq.

5.3 Experimental setup

In real life, pedestrian radiation portals usually are made in a form of letter "П": ~2 m wide and ~3 m high. Of course, there are different configurations, depending on amount of detectors and their' sizes, but in one of the most simple and widespread configuration there are 2 detectors that are placed in a distance ~2 m from each other at ~1 m from the floor. It means that the maximal distance from any

detector to the path of gamma radiation source that may pass through the portal is equal or less than 1 meter. Thus, if we wish to make a simulation of real life situation with only 1 detector, then the distance between source path and detector should be the same.

In order to simulate the passing of human with source of gamma radiation, for following experiment setup was made. The detector was placed vertically on a table (height of the table was ~75-78 cm), distance from the detector to the nearest wall ~50 cm, to the other walls — more than 3 m.

Natural background radiation coming from a 70 kg person is typically ~7.4 kBq (4400 Bq of K-40 and 3000 Bq of C-14), the average activity from K-40 in Earth's crust is 850 Bq/kg, and maximum prohibited activity of any material (by International Atomic Energy Agency) is between 100 Bq/kg (pure Ac-227) and 10 GBq/kg (pure Ar-39) depending on mix of radioactive elements ([7], [8]).

For pure Co-60 maximal permitted total activity for ordinary materials is 100 kBq and for Cs-137 this value is 10 kBq [8].

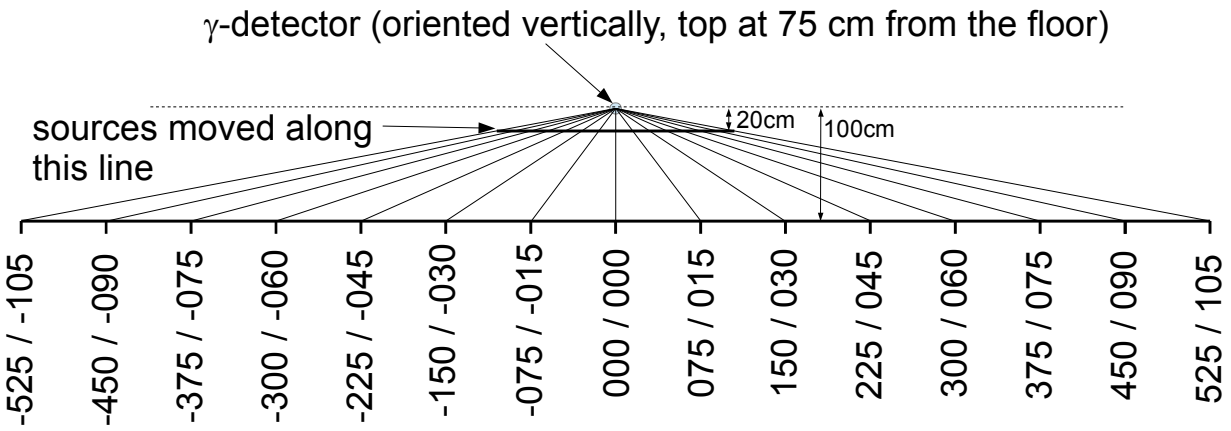

Figure 3. Schematic view of the measurement geometry.

Figure 3 shows the schematic geometry of the experiment. There are 2 important axes: vertical (Y) and horizontal (X). Due to low activity of available gamma sources (~8 and ~29 kBq), the distance from detector to the path (axis Y at point 0) of source was decreased 5 times: from 1 m to 20 cm. The relation between radiation intensity and distance is $I \sim 1/R^2$, which allows us to simulate 25 times stronger activity on the path with distance 1 m from the detector.

Also, in order to keep the geometry the same, horizontal axis X is also decreased 5 times. Measurements with Cs-137 and Co-60 sources were done at 15 points, with Y = 20 cm (distance between detector and path of source) and dX = 15 cm (distance between points for measurements). 10 measurements were done at each point; duration of each measurement was 1 second.

In total, for each source 3 various series of experiments were done (2 elements*3 series*15 points*10 measurements = 900 measurements in total):

1. Pure source. In this case, there is only source and detector with no obstacles between them.

2. Source and bottle. Source is attached to 5 liter plastic bottle filled with water, which simulates a body of human that tries to pass the detector with gamma source in the "back" pocket. It means that the source always have the correct position (exactly in the point of measurements), and is attached to the "back" of the bottle ("human"): in negative positions gamma rays has to pass through the bottle to reach the detector, but in positive positions there are no obstacles between them.

3. Source with lead shielding. In this case, there is 0.5 mm thick lead shield between the source and the detector (at distance ~3 cm from the source).

Photographs of the experiment are available at Appendix B.

5.4 Data analysis procedure

The ultimate goal of the data analysis was to detect a radioactive source while the person is walking through the portal. The detection is based on the analysis of the signal to noise ratio (SNR), where the signal is the total number of detected gamma-rays from the radioactive source, and the background is the total number of detected gamma-rays coming from natural background. So, in our case the SNR can be referred to as signal-to-background ratio.

Radioactive decay is a random process. It is not possible to say when an unstable nucleus will decay, only that it will decay with certain probability within certain period of time. Natural background follows Poisson distribution:

$$P(k)=\frac{\lambda^k e^{-\lambda}}{k!} \quad (4)$$

where P(k) is the probability that k events will happen within some time interval (e.g. one second), and λ is the mean number of events per this time interval.

For sufficiently large values of λ the normal distribution with mean λ and variance λ (standard deviation $\lambda^{1/2}$) becomes a good approximation to the Poisson distribution.

The probability that we will get a particular count rate can be approximated by a Gaussian (or normal) distribution: ([4], pp. 41-46)

$$f(x) = \frac{1}{\sigma\sqrt{2\pi}} \times e^{\frac{-(x-\mu)^2}{2\sigma^2}} \quad (5),$$

where μ is mean of the distribution and σ is standard deviation.

In a Poisson process, the number of observed occurrences fluctuates about its mean λ with a standard deviation

$$\sigma_k = \sqrt{\lambda} \quad (6).$$

Thus, in radioactivity detection portal the criterion for the detection is usually taken to be:

$$N_{effect} > n * \text{sqrt}(N_{background}) \ (7),$$

where n is a parameter corresponding to the required SNR, and N_{effect} and $N_{background}$ are the number of gamma-rays detected form the radioactive source and the natural background respectively.

The parameter n is directly connected to the expected number of false alarms that the system would produce due to accidental excess in the number of detected gamma-rays. The integral of the normal distribution from n to infinity (quantile) equals the probability that the detected number of gamma-rays will exceed the mean by n standard deviations. Picture below illustrates the shape of normal distribution (μ = 0, σ = 1). Green lines show us various sigma levels: for example, the area under the peak in segment [1, ∞] is equal to 0.159, which translates into about 16% probability that the SNR in the given measurement will exceed the one-sigma threshold.

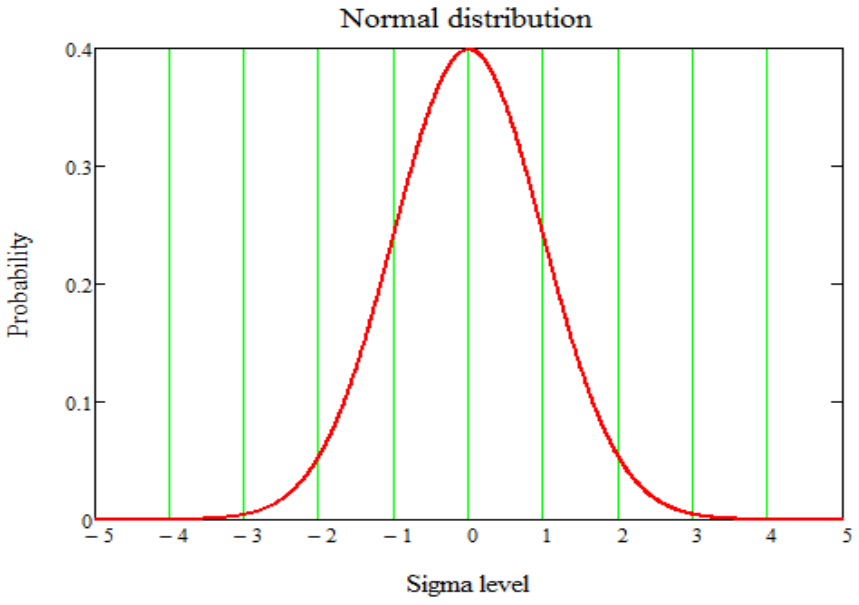

Illustration of a normal distribution.

For reasonable number of false alarms produced by a radiation portal is of the order of one per day. This translates into the requirement that SNR ≥ 5, so the “five-sigma” rule was chosen as the target in this work.

5.5 Experimental results

Due to low activity and small time of each measurement (1 second, which is dictated by the typical speed with which the person would pass through the radiation portal), the measured spectra have very low statistics. It means that at points with maximal distance from the detector (points 105 cm and -105 cm) the contribution from the source is very weak, so we can assume that the detector is measuring pure background. Even at closest best positions (points -15 cm and 15 cm) there are not too many events under the peak integral. Figure 4 and Figure 5 illustrate typical measurement results for pure Co-60 at the farthest and the closest points of the trajectory.

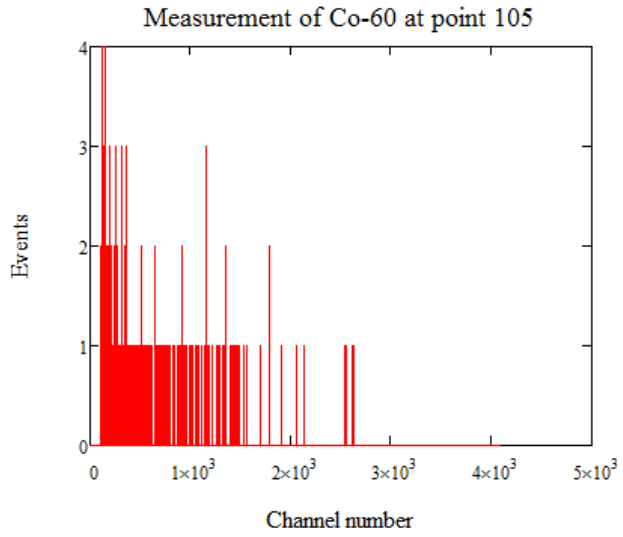

Figure 4. Example of a spectrum of Co-60 measured in 1 second at the farthest point of the trajectory.

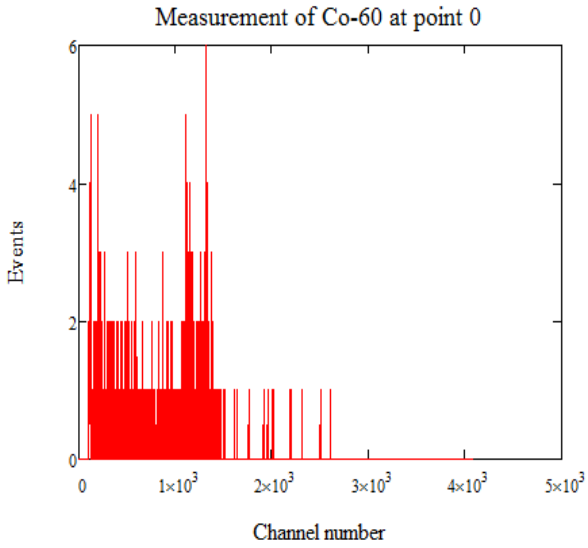

Figure 5. Example of a spectrum of Co-60 measured in 1 second at the closest point of the trajectory.

So, in all further calculations, measurements at point -150 cm and 150 cm were assumed to be pure background. There was 2 different methods to find the final result (both use same formulas): “mean” method and “finer” method. The first one was used to receive general picture and second one was used to receive precise results with lower uncertainty.

5.5.1 Results provided by “mean” method

The main idea of this method was to find mean value for every single measurement, its statistical uncertainty (so called A-type uncertainty, because B-type uncertainty is unknown) and degree of freedom for further calculations.

First of all, it was necessary to find necessary channels for peak detection. For that propose, all 10 measurement results of “pure source” series at point 0 was summed. Co-60 has strong gamma lines at ~1173 keV and ~1333 keV, while Cs-137 has strong line at 662 keV. Knowing that 1 channel number ~ 1 keV (but NOT EQUAL!) and comparing it with background spectra, it is possible to find necessary intervals. Figure 6 and Figure 7 show the result (red color shows spectrum of the corresponding isotope, blue color shows the background).

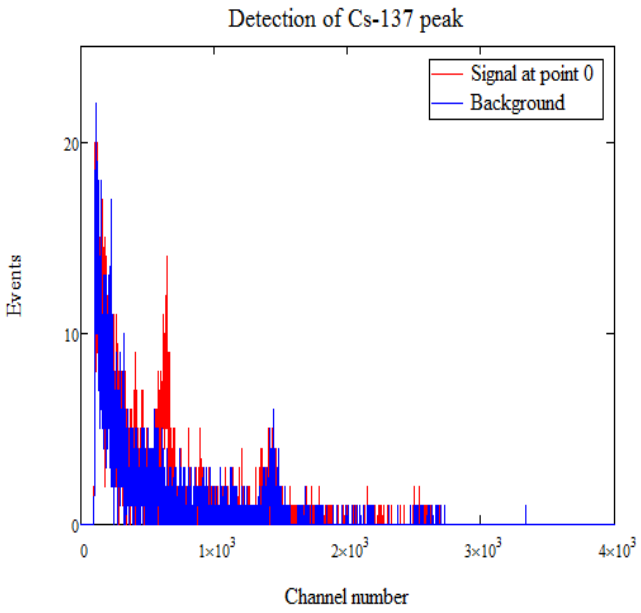

Figure 7. Comparison of the spectrum of Cs-137 with the background.

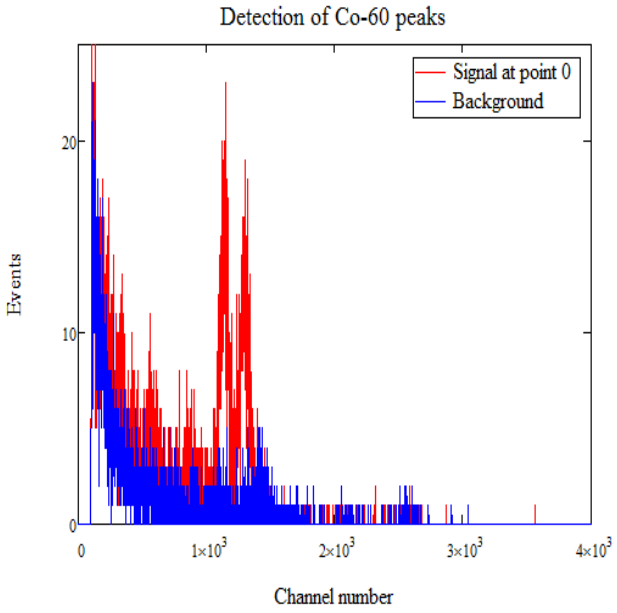

Figure 6. Comparison of the spectrum of Co-60 with the background.

Simple analysis of received spectra allows to locate necessary channels (necessary area under the peak was at FWHM (full width at half maximum)): [1093-1175] and [1246-1347] for Co-60 and [616-664] for Cs-137.

In order to find mean value of background, we sum all events (x) in necessary channels [a; b] for all background measurements and then divide it on number of measurements in this point (N). Due to absence of information about B-type uncertainty, we may use only experimental standard deviation of the mean (A-type uncertainty) to form total uncertainty. Also, we may say that degree of freedom ν is equal to N – 1.

$$B=\frac{\sum_{j=1}^{N}\sum_{i=a}^{b}x_{i,j}}{N} \qquad u_A(B)=\sqrt{\frac{\sum_{j=1}^{N}\left(\sum_{i=a}^{b}x_i-B\right)_j^2}{N(N-1)}} \quad (8), (9)$$

Same formulas may be be applied to find average value of signal at any point, its uncertainty and degree of freedom. The only difference is in number of measurements – for background we have 2 points (-105 and 105) with N = 10 + 10 = 20; and for the rest positions calculations are done for each point separately (N = 10). Of course, in formula for A-type uncertainty we should use average value of signal at this point instead of B.

The next step was to find σ values in each point. From theoretical part we know that sigma is directly proportional to ratio of pure signal (S – B) to background, so:

$$\sigma=\frac{S-B}{\sqrt{B}} \qquad u_C(\sigma)=\sqrt{\left(\frac{d(\sigma)}{dS_i}u_A(S)\right)^2+\left(\frac{d(\sigma)}{dB}u_A(B)\right)^2} \quad (10), (11)$$

$$\nu_{eff}=\frac{u_C(\sigma)^4}{\frac{\left(\frac{d(\sigma)}{dS_i}u_A(S)\right)^4}{\nu_S}+\frac{\left(\frac{d(\sigma)}{dB_i}u_A(B)\right)^4}{\nu_B}} \quad (12)$$

where u_C is combined uncertainty of sigma and ν_{eff} is effective degree of freedom for σ that are used to obtain expanded uncertainty (U) that is giving a coverage interval for sigma with specified probability:

$$U(sigma)=t\cdot u_C(sigma) \quad (13)$$

So in our case, t is coverage factor of Student's t test, that depends on effective degree of freedom and specified probability (in our case p = 95%). In all calculations the received value of $\nu_{eff} = 1$, which means that if p=95, t = 12.71. [9]

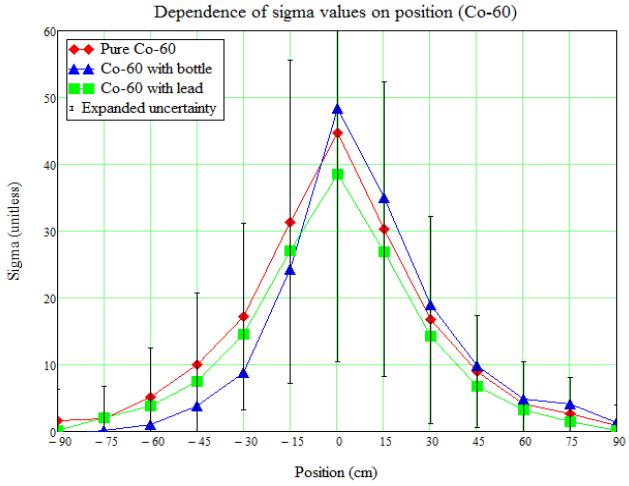

Figure 8. Dependence of the number of "sigmas" on the Co-60 source position along the trajectory.

Figure 8 illustrates results of calculating sigma values for Co-60. As we may see, the smallest value of expanded uncertainty (pure Co-60) is extremely high. The only useful information that may be obtained from this data is that the maximal sigma valueis located at point 0 (where pure signal is the strongest) and that only points [-30; 30] have more or less good signal, all the rest are not suitable, because signal there is not very different from background noise. Situation with Cs-137 is even worse. Graphs for Cs-137 are available in Appendix C (on those graphs only ordinary uncertainty is available, but it is not hard to understand that by multiplying them with t = 12.71 we will receive absurd answers).

5.5.2 Results provided by “finer” method

“Mean” method provided us with too bad statistics, so different approach was applied – so called “finer” method. From *data analysis procedure* chapter we know that radioactive decay is a random event, and hence that all measurements in all positions are completely independent. It means that in order to find sigma value in a certain position, we may try to combine all measurements in that point with all background measurements. The following formula defines mean value of σ for position n with new method (j = 1 … 10; k = 1 … 20; x^n = events of 1 measurement at position n; y - events of 1 background measurement):

$$\sigma_n = \frac{\sum_{m=1}^{j*k} \left(\frac{\sum_{i=a}^{b} x_{i,j}^{n} - \sum_{i=a}^{b} y_{i,k}}{\sqrt{\sum_{i=a}^{b} y_{i,k}}} \right)^m}{j*k} \quad (14)$$

In other words, we may say that in order to find good mean σ value, we have to:

1. Find sum of events (x) at necessary channels [a; b] for the first measurement at this position (n) and to subtract from this number sum of background events (y) at necessary channels [a; b] from the first background measurement. Then we have to divide received number by square root of sum of background events (y) at necessary channels [a; b] from the same first background measurement. This will provide us with first σ value.

2. Repeat step 1 with all the rest measurements (from 2-nd to 10-th) at this position (n) with the same first background. This will provide us with first 10 (j = 1 … 10) σ values.

3. Repeat step 1 and 2 with all the rest (from 2-nd to 20-th, because k = 1 … 20) background measurements at this position (n). This should provide us with 200 different σ values (10*20 = 200).

4. Find mean value from received 200 σ values (their sum divided by their number).

Step 3 provided us with 200 different independent σ values, so now it is possible to find experimental standard deviation of the mean (A-type uncertainty) and degree of freedom for mean σ value at point n:

$$u_A(\sigma)=\sqrt{\frac{\sum_{m=1}^{j*k}(\sigma_m-\bar{\sigma})^2}{j\cdot k(j\cdot k-1)}}\ ,\quad \nu=j\cdot k-1 \qquad (15), (16)$$

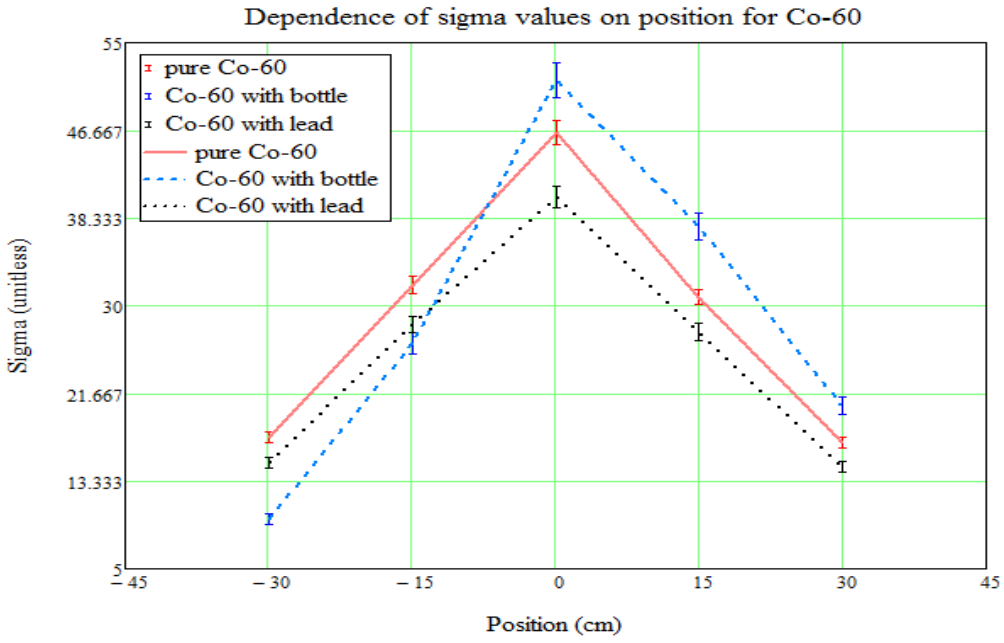

Figure 9. Dependence of the number of "sigmas" on the Co-60 source position along the trajectory in the "finer" method.

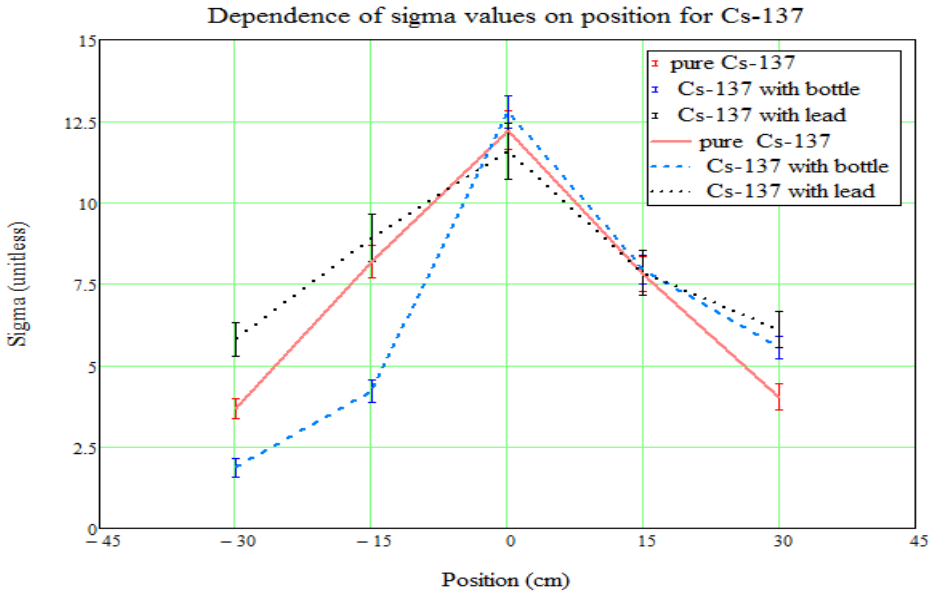

Figure 10. Dependence of the number of "sigmas" on the Cs-137 source position along the trajectory.

Figure 9 and Figure 10 illustrate the results of "finer" method. As we may see, this time expanded uncertainties are much better and it is possible to continue calculations with those results.

Also, those graphs illustrate very well one interesting effect - the scattering of gamma photons. The main idea of this effect is that if we will try to protect the detector with too thin layer of shielding material then we may receive even stronger signal (in case of human body – bigger dose) than without shielding. It happens because photons that originally were not moving into the detector (or human body) change their direction after scattering and due to the fact, that layer of shielding material is too thin and cannot significantly decrease their energies, those photons are hitting the target that they should not hit without shielding (see Figure 11). This effect is working not only with objects between detector and source, but also with nearby objects. In both Figure 9 and Figure 10 sigma values (situation with bottle of water) at positions -30 and are shielded by bottle with water, but when source is passing points 0, 15 and 30, some of photons that were moving into direction of bottle (not direction of the detector) change their trajectory and in the end hit the detector. This is the reason why under certain conditions we have even better σ results than with pure source.

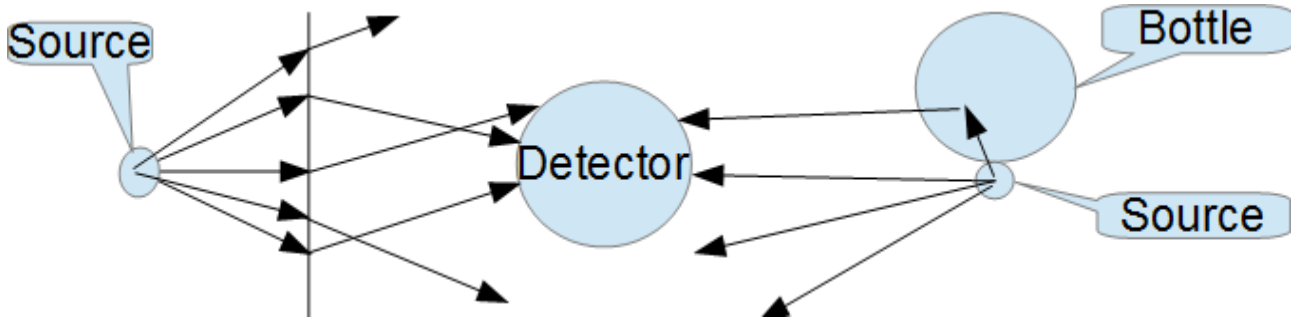

Figure 11. Illustration of shielding effect. Arrows show possible photon trajectory.

However, received results may not able to provide us with best answer, because source should be moving with speed 5 km/h. It means that we may sum measurements in some positions to receive the best answer. Knowing that

$$5 \text{ km/h} = 1.389 \text{ m/s} \leq 1.5 \text{ m/s} = 150 \text{ cm/s}, \quad (17)$$

it is possible to assume that with this speed source will move though points [-30; 30] for 2 seconds. Other positions are not so important, because we have to find minimal detection activity of the detector, and as we may see from previous results, the maximal detection ability is located at position 0 and is gradually decreasing when source is moving in any direction from this point (backward or forward). In other words, the detector have to detect something when source is passing through it, but not when source is still far away.

Due to the fact, that motion of the source is linear and has constant velocity, there are 3 position combinations in region [-30; 30] that will allow to find necessary σ value: -30 and 0; -15 and 15; 0 and 15. However, -30 and 0 is more preferable than 0 and 30, because in that case detection will provide

alarm right after the source passed through the portal, and not when it is 1.5 m away from it (point 30 = 150 cm from the portal, source moves from position -30). Instead of simple summation of 2 sigma values, it is necessary to use formula _ to find 1 mean value of σ from 2 positions, because during measurement of gamma spectrum background will also increase (in our case, it will increase 2 times):

$$\sigma_{1+2} = \frac{\sum_{m=1}^{j*k} \left(\frac{\sum_{i=a}^{b} x_{i,j}^{1} + \sum_{i=a}^{b} x_{i,j}^{2} - 2 \cdot \sum_{i=a}^{b} y_{i,k}}{\sqrt{2 \cdot \sum_{i=a}^{b} y_{i,k}}} \right)^{m}}{j*k} \quad (18)$$

Here x^1 means measured events at first position (-30 or -15, depending on the pair) and x^2 means measured events at second position (0 or 15). All the rest is the same as in σ calculation for single position (including uncertainty and degree of freedom calculation). Following table shows results for new calculations comparing them with old results for point 0:

Comparison of results for different integration times and positions							
Source	Integration time (pos.)	Pure source		Source with bottle		Source with lead	
		Sigma	Uncertainty	Sigma	Uncertainty	Sigma	Uncertainty
Co-60	1 s (0)	**46,46**	0,57	**51,4**	0,85	**40,32**	0,52
	2 s (-30, 0)	45,2	0,5	43,21	0,77	39,2	0,52
	2 s (-15,15)	44,39	0,52	45,2	0,79	39,39	0,54
Cs-137	1 s (0)	**12,22**	0,31	**12,77**	0,25	11,58	0,43
	2 s (-30, 0)	11,24	0,3	10,35	0,26	**12,3**	0,47
	2 s (-15,15)	11,32	0,32	8,6	0,23	11,86	0,47

As we can see, for all situations except Cs-137 and 0.5 mm lead shielding, the best σ value is always 1 second measurement in position 0. It means, that for further calculations we should take this value.

As it was mentioned in *experimental setup* part, distance between real detector and source at point 0 is 5 times greater than during the experiment. Thus, it is possible to say that received values of sigma are true for source with activity 25 times greater, than during the experiment. So, we may imagine a graph, where Y axis shows minimal detection activity (MDA) in kBq and X axis represents necessary sigma level for detection of activity given by Y axis. In that case, it is possible to add on the graph received results: for example for Co-60 with activity 695.63 (27) kBq (25*8.81 = 695.63) corresponding σ value is 46.46. Also, we may say that at point X = 0, Y=0. It means that absolutely any measurement will cause alarm state, even if there is no gamma source (detector will detect background as a source). Knowing that dependence of MDA on σ is linear (MDA = a*σ, where "a" is slope), it is easy to make necessary calculations to find MDA for necessary σ level:

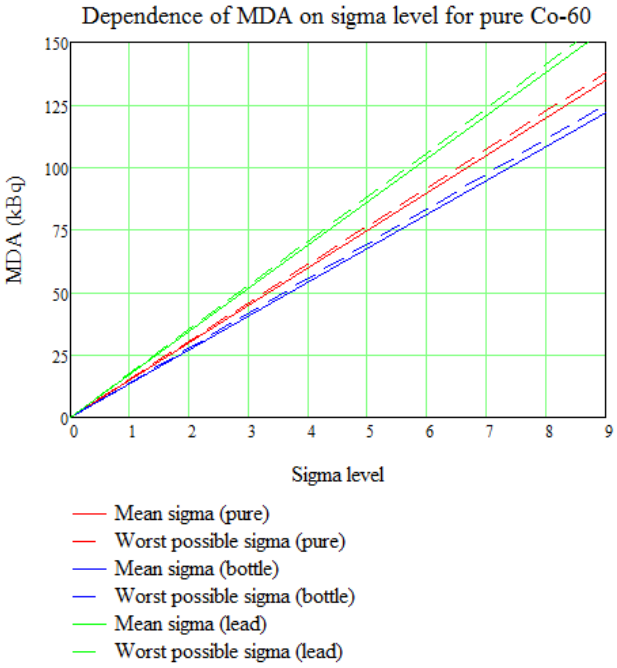

Figure 12. Dependence of MDA on sigma level for C0-60.

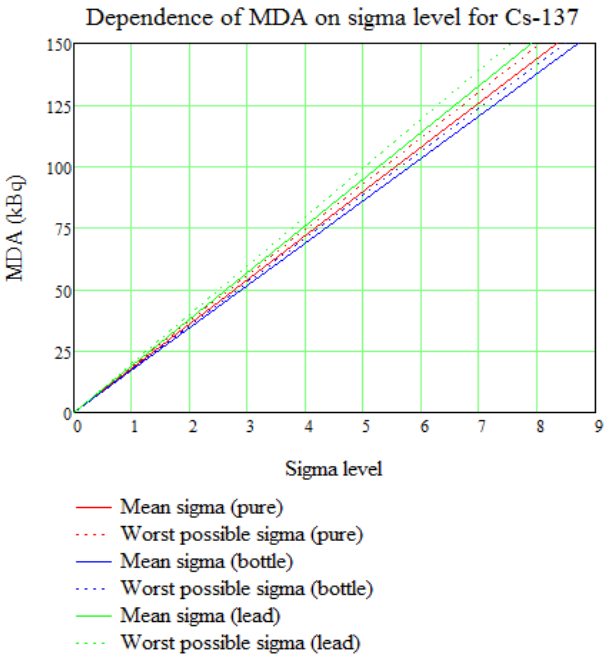

Figure 13. Dependence of MDA on sigma level for Cs-137.

Figure 12 and Figure 13 show dependence of MDA on sigma level in necessary region. Dotted lines show the worst possible MDA values (maximal activity (activity + uncertainty) with minimal sigma level (sigma level - uncertainty) and ordinary lines show calculated values of activity and sigma level. Difference between dotted and ordinary line provide us with uncertainty of MDA.

The following tables shows the necessary MDA for first 8 sigma levels (U means expanded uncertainty with probability 95%, and with degree of freedom jk – 2, because we are including point 0.0 with slopes; but it is not very important, because in our case jk ~ (jk – 1) ~ (jk – 2)). In order to have less than 1 detection per 24 hours, we need $\sigma \geq 5$.

Sigma level	MDA for Cs-137 (kBq)					
	pure		bottle with water		0,5 mm lead shielding	
	Average	U	Average	U	Average	U
1	18	2	17	1	19	2
2	36	3	34	2	38	4
3	54	4	52	3	57	6
4	72	5	69	4	76	8
5	90	7	86	5	95	9
6	108	8	103	6	114	11
7	126	9	121	7	133	13
8	144	10	138	8	152	15

The results show that minimal detection ability of only 1 BGO detector is enough to detect minimal activity of Co-60 that is not dangerous to environment determined by IAEA norms (100 kBq), and is not enough to detect minimal activity of Cs-137 (10 kBq).

Sigma level	MDA for Co-60 (kBq)					
	pure		bottle with water		0,5 mm lead shielding	
	Average	U	Average	U	Average	U
1	15	1	14	1	17	1
2	30	2	27	2	35	2
3	45	2	41	3	52	3
4	60	3	54	3	69	4
5	75	4	68	4	86	4
6	90	4	81	5	104	5
7	105	5	95	5	121	6
8	120	6	108	6	138	7

6 References

[1] R.T. Kouzes, J.H. Ely, B.D. Milbrath, J.E Schweppe, E.R. Siciliano, D.C. Stromswold. "Spectroscopic and Non-Spectroscopic Radiation Portal Applications to Border Security" in *"IEEE Nuclear Science Symposium Conference Record"* (2005), (Volume: 1), 0-7803-9221-3, pp. 321 – 325

[2] Andrey Kuznetsov. *Extending Security Perimeter and Protecting Crowded Places with Human Security Radar.* (APSTEC, 2015)

[3] Syed Naeem Ahmed. *Physics and engineering of radiation detection.* First edition (Academic Press, 2007)

[4] Jeff C. Bryan. *Introduction to nuclear science.* Second edition. (CRC Press, 2013)

[5] H. Schubert, A. Kuznetsov, *Detection of Liquid Explosives and Flammable Agents in Connection with Terrorism*, St.-Petersburg, Russia, October 17-19, 2007 (Springer) pp. 71-78

[6] P. Lecoq, A. Annenkov, A.Gektin, M. Korzhik, C. Pedrini. *Inorganic scintillators for detector systems*. (Springer 2006)

[7] *Naturally-occurring radioactive materials (NORM).* World Nuclear Association (2015) http://www.world-nuclear.org/information-library/safety-and-security/radiation-and-health/naturally-occurring-radioactive-materials-norm.aspx

[8] *Regulations for the safe transport of radioactive material.* IAEA (2012) http://www-pub.iaea.org/MTCD/publications/PDF/Pub1570_web.pdf

[9] Rein Laaneots, Olev Mathiensen, Jurgen Riim. *Metroloogia. Õpik kõrgkoolidele.* (TTÜ kirjastus, Tallinn 2012)

7 Lihtlitsents lõputöö reprodutseerimiseks ja lõputöö üldsusele kättesaadavaks tegemiseks

Mina, Andrei Kovaljov,

1. annan Tartu Ülikoolile tasuta loa (lihtlitsentsi) enda loodud teose *DEVELOPMENT OF METHOD FOR DETERMINATION OF MINIMAL DETECTION ABILITY OF BISMUTH GERMANIUM OXIDE GAMMA DETECTOR*, mille juhendajad on Alan Henry Tkaczyk ja Dmitrii Vakhtin,

    1. reprodutseerimiseks säilitamise ja üldsusele kättesaadavaks tegemise eesmärgil, sealhulgas digitaalarhiivi DSpace-is lisamise eesmärgil kuni autoriõiguse kehtivuse tähtaja lõppemiseni;

    2. üldsusele kättesaadavaks tegemiseks Tartu Ülikooli veebikeskkonna kaudu, sealhulgas digitaalarhiivi DSpace´i kaudu kuni autoriõiguse kehtivuse tähtaja lõppemiseni.

2. olen teadlik, et punktis 1 nimetatud õigused jäävad alles ka autorile.

3. kinnitan, et lihtlitsentsi andmisega ei rikuta teiste isikute intellektuaalomandi ega isikuandmete kaitse seadusest tulenevaid õigusi.

Tartu, 27.05.2016

8 Appendix A

In the following table are listed only those isotopes that have at least 1 strong line with E=200 keV. The only exception to this rule are nuclear materials (U and Pu isotopes). Also, *critical activity* (this level of activity of *special sources* and more is dangerous for environment) is given only for medical isotopes, whose detection is recommended by IAEA (International Atomic Energy Agency).

Types of radioactive materials:	
NORM	Naturally Occurring Radioactive Materials
MED	medical radioactive materials
IND	industrial radioactive materials
NUC	nuclear radioactive materials

#	Categories:
1	Easily detectable (strong lines with E > 500keV)
2	Barely detectable (no strong lines with E > 500keV, strong lines at E>300keV)
3	Almost undetectable (no strong lines with E > 300keV)
4	Undetectable (no strong lines with E > 50keV)

#	Isotope	Type	Category	Comments
1	K-40	NORM	1	
2	Co-60	MED/IND	1	Critical activity - 30 GBq.
3	Ga-67	IND	2	May be in category 3 - the only good detectable line has E = 300 keV.
4	Se-75	IND	2	May be in category 3, line 400 keV is not very good, but lines 264 and 279 keV are better.
5	Kr-85m	MED	2	May be in category 3 - the only good detectable line has E = 304 keV.
6	Mo-99	MED	2	Critical activity - 300 GBq.
7	In-111	MED	3	
8	Sb-124	IND	1	
9	I-131	MED	2	Critical activity - 20 GBq.
10	Xe-133m	MED	3	Usually Xe-133 is being used, which in not detectable with our detector.
11	Cs-137	MED/IND	1	Critical activity - 100 GBq.
12	Eu-152	IND	1	Gamma spectra has a lot of lines.
13	Eu-154	IND	1	Gamma spectra has a lot of lines.
14	Yb-169	IND	2	May be in category 3 - the only good detectable line has E = 308 keV.
15	Ir-192	MED/IND	2	Critical activity - 80 GBq.
16	Au-198	MED	2	Critical activity - 60 GBq.
17	Tl-208	NORM	1	Th-232 decay chain.
18	Bi-210m	NORM	2	U-238 decay chain, may be in category 3 - good lines are 266 keV and 304 keV.
19	Pb-212	NORM	3	Th-232 decay chain.
20	Bi-214	NORM	1	U-238 decay chain.
21	Pb-214	NORM	2	U-238 decay chain.
22	Ac-228	NORM	1	Th-232 decay chain.
23	Pa-234	NORM	1	U-238 decay chain.
24	U-235	NUC	3	
25	U-238	NUC	4	
26	Pu-239	NUC	4	
27	Pu-240	NUC	4	
28	Pu-241	NUC	4	

9 Appendix B

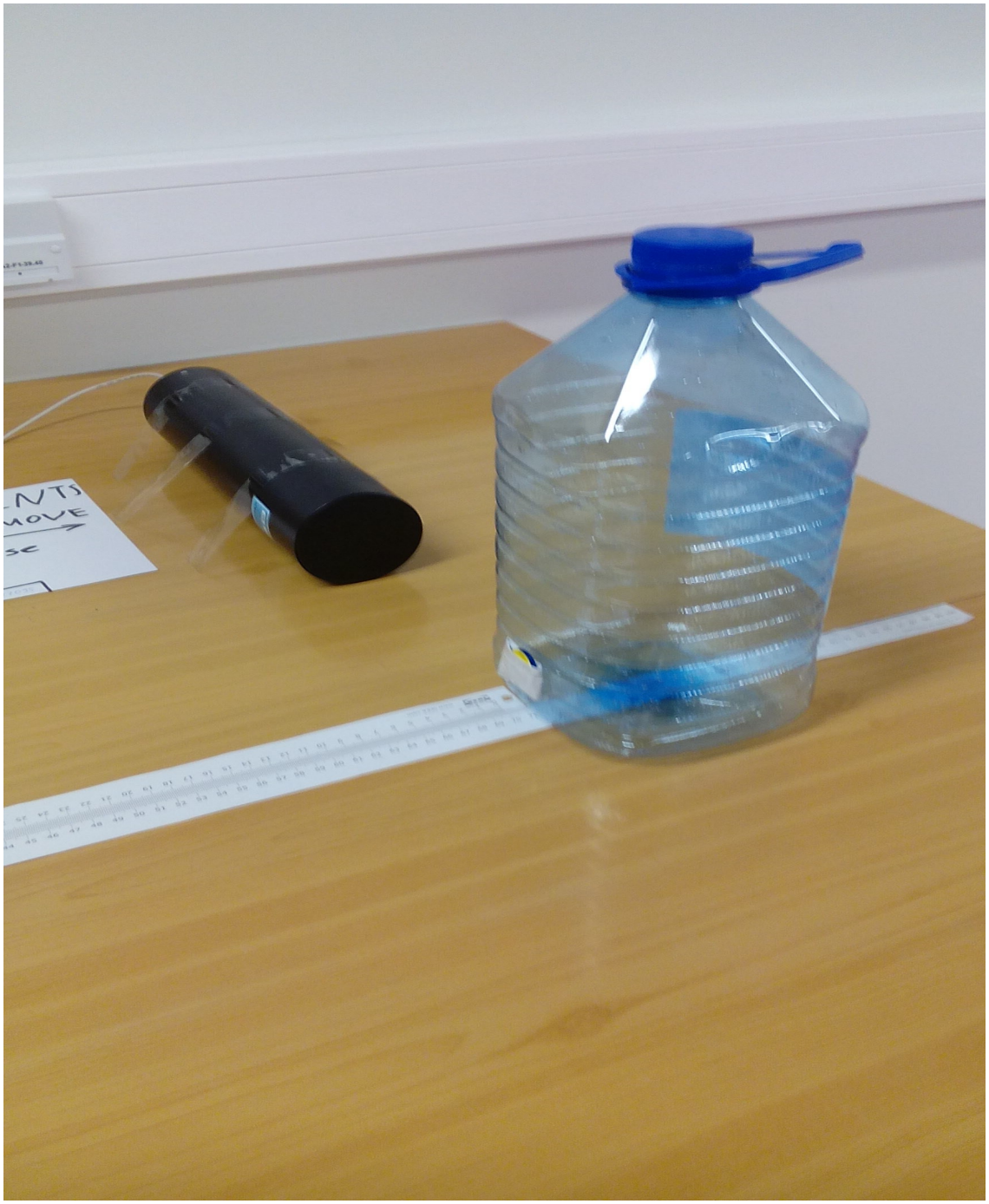

10 Appendix C